EUROPEAN JOURNAL OF REMOTE SENSING, 2017
VOL. 50, NO. 1, 1328646
https://doi.org/10.1080/22797254.2017.1331117

Taylor & Francis
Taylor & Francis Group

Sea-ice area variability and trends in Arctic sectors of different morphology, 1996–2015

Mauro Boccolari[a] and Flavio Parmiggiani[b]

[a]Department of Chemical and Geological Sciences, University of Modena and Reggio Emilia, Modena, Italy; [b]ISAC–CNR, Bologna, Italy

ABSTRACT

This study presents a comparison of the sea-ice cover of the whole Arctic Ocean with two arctic sectors of different morphology: the Greenland Sea, as a typical "open sea", and the Beaufort Sea, as a typical "closed sea". The study refers to the period January 1996–December 2015 and makes use of the Arctic sea-ice concentration data set produced, on a daily basis, by the Institute of Environmental Physics of the University of Bremen. From the whole Arctic data set, two subsets, covering the Greenland Sea and the Beaufort Sea, were extracted. The extent of sea-ice cover was obtained by the sea-ice area (SIA) parameter, which was computed according to the conventional NASA method. Our analysis shows that the strong summer decline of the Arctic SIA in the last 20 years is not observed in the Greenland Sea (the trend of SIA minimum values is 0.7 ± 2.010^3 km^2 year^{-1}) while it is even greater in the Beaufort Sea.

ARTICLE HISTORY
Received 31 January 2017
Revised 2 May 2017
Accepted 12 May 2017

KEYWORDS
Sea ice area; Arctic; Beaufort Sea; Greenland Sea

Introduction

Several studies, carried out since the end of twentieth century (Parkinson, Cavalieri, Gloersen, Zwally, & Comiso, 1999; Toudal, 1999; Vinnikov et al., 1999), and in more recent years (Cavalieri & Parkinson, 2012; Comiso, 2012; Comiso & Nishio, 2008; Comiso, Parkinson, Gersten, & Stock, 2008; Meier, Stroeve, & Fetterer, 2007; Parkinson & Cavalieri, 2008; Stroeve et al., 2012; Vinnikov, Cavalieri, & Parkinson, 2006), have shown a generalized, significant decline in Arctic ice cover, i.e. sea ice extent and area, in the last 30 years. Comiso and Nishio (2008), using the combination of high-resolution AMSR-E data with SSM/I and SMMR data, found that maximum reduction occurred in 2007, a reduction slightly compensated after 2008 (Comiso, 2012), but afterwards followed, in 2012, by a new stronger summer record minimum (Comiso & Hall, 2014). Recent reviews analysing Arctic sea-ice cover decline (Liu, Key, & Wang, 2009; Stroeve et al., 2012; Wang et al., 2012) have investigated the relevant sea-ice forcing mechanisms.

In this paper, the annual cycle of sea ice area (SIA) distribution in the whole Arctic Ocean has been analysed for the period January 1996–December 2015 and compared with what happened, in the same period, in two sectors of the Arctic of different morphology, the Greenland Sea, a typical "open sea", and the Beaufort Sea, a typical "closed sea". While being well aware that sea-ice cover depends on several physical factors (low temperatures, persistence of a surface fresh water layer, inflow of low salinity water through the Bering Strait etc.) (Serreze & Barry, 2014), the aim of this study was to investigate trend differences between two seas of different morphology of the Arctic Ocean. This result seems to confirm the hypothesis of King (2014) which tries to explain the different degrees of sea-ice decline in the Arctic and Antarctic regions: in the Arctic Ocean, where the ice is mostly confined by the surrounding continents, the summer ice is dramatically decreasing, while in Antarctica, where the sea ice is largely free to drift with the wind and ocean currents, the ice is growing.

Data and methods

The IUP data set

The study was carried out using the daily Arctic sea-ice concentration (SIC) data set produced by the Institute of Environmental Physics (IUP) of the University of Bremen. SIC data were derived from the observations of SSM/I, SSMIS, AMSR-E and AMSR-2 passive microwave sensors by using the ARTIST Sea Ice (ASI) algorithm (Kaleschke et al., 2001; Spreen, Kaleschke, & Heygster, 2008), based on 89 GHz brightness temperature values distributed by NSIDC and by JAXA. The SSMIS data set was only used to fill the gap between AMSR-E and AMSR-2. All SIC data are mapped by IUP onto a stereo-polar grid having a pixel of 6.25 km. From the Arctic data set, two subsets covering the Greenland Sea, approximately from 57.1 N to 83.5 N and from 41.4 W to 14.9 E, and the Beaufort Sea, approximately from 80.4 N to 66.5 N and from 116.6 W to 184.3 W, were

CONTACT Flavio Parmiggiani f.parmiggiani@isac.cnr.it ISAC–CNR, Via P. Gobetti 101, Bologna 40129, Italy
Supplemental data for this article can be accessed here.

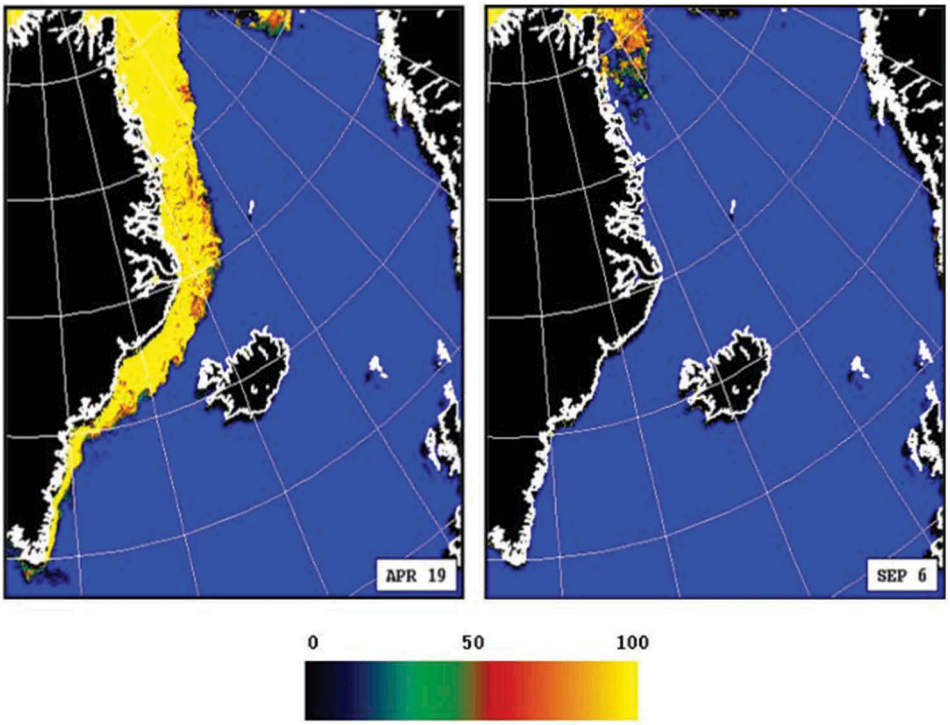

Figure 1. SIC (%) in the East Greenland Sea. Left: near the peak of the freezing season (19 April 2013). Right: near the peak of the melting season (6 September 2013).

extracted (see Figures 1 and 2). These two regions, together with the whole Arctic Ocean, are our regions of interest (ROIs) (Figure 3).

Hereafter, the three study areas will be identified as ROI1 (the Arctic Ocean as a whole), ROI2 (the Greenland Sea) and ROI3 (the Beaufort Sea). As the sensors do not cover a small circular zone around the North Pole, for the full Arctic region, a constant value of 100% SIC was added to fill the hole. With reference to the AMSR-2 product, the surface area of the three ROIs is approximately 85, 2.6 and 2.0 M km^2, respectively.

Building the monthly SIA time series 1996–2015

Given N grid cells the SIA is conventionally defined as

$$\mathrm{SIA} = \sum_{i=1}^{N} \mathrm{SIC}_i A_i$$

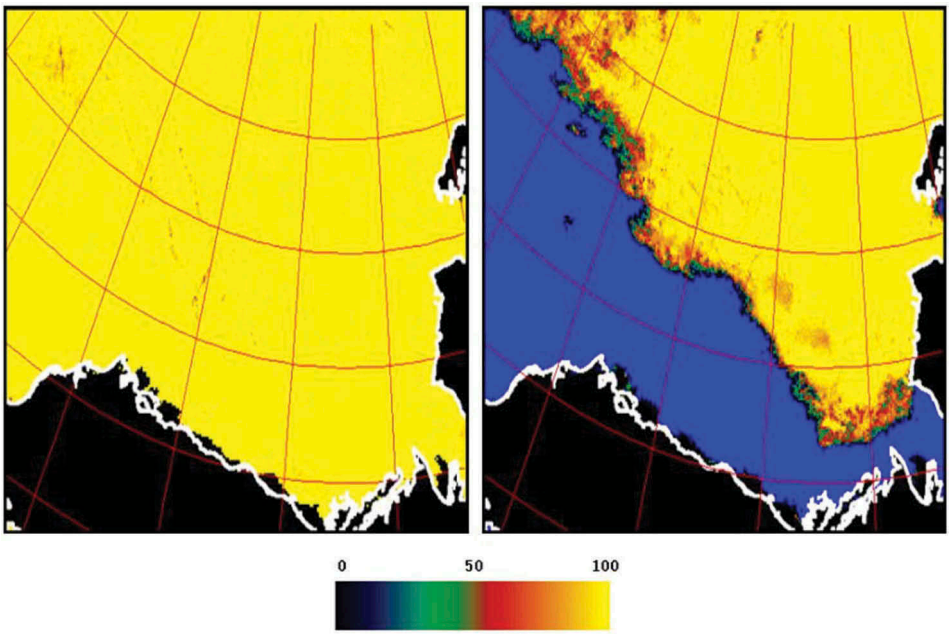

Figure 2. Same as Figure 1 for the Beaufort Sea.

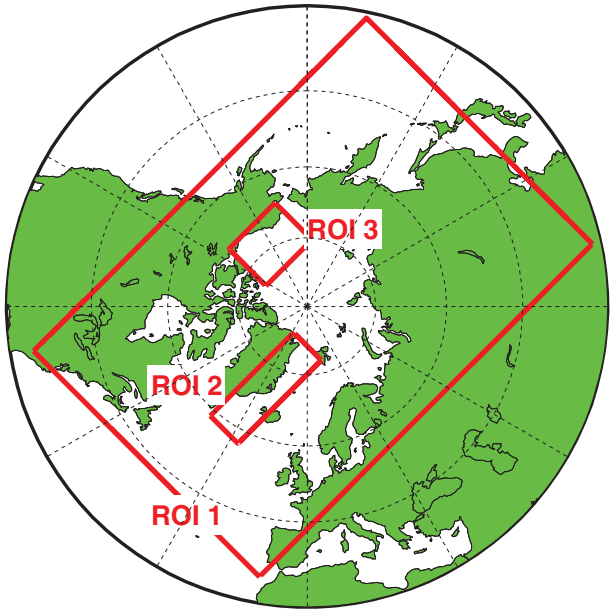

Figure 3. Location of the three regions of interest (ROIs).

where SIC_i and A_i are, respectively, the sea-ice concentration and the surface area of the ith grid cell. In addition, the sum only takes into account the cells having SIC ≥ 0.15 (Zwally et al., 1983). After SIA estimation, an outlier-removing method, based on the distance of the points from the running mean of the series, was applied. The percentage of outliers for each ROI was 0.3%, 2.2% and 0.4%, respectively, with the highest values occurring for the SSM/I and SSMIS series. The next step was to put together the SIA time series derived from different satellite sensors. Due to the different spatial resolution between SSM/I and the AMSR data, a slight difference between the SIA as measured by the two sensors is to be expected.

The consistency between SSM/I and AMSR-E data sets was obtained by normalizing the SSM/I data set by means of parameters derived using a linear regression of the data from the two sensors during the period of overlap. In Comiso and Nishio (2008), the normalization was applied to the brightness temperature of each channel, but in this work, a linear regression model was simply applied to SIA:

$$A_{\mathrm{AMSR-E}} = c_0 + c_1 \mathrm{SIA}_{\mathrm{SSM/I}} \quad (1)$$

In Table 1, the regression coefficients, c_0 and c_1, together with the mean-area difference, md, and the standard deviation, sd, between the two daily products (SSM/I and AMSR-E) for the overlapping period, that is

$$\mathrm{md} = \overline{\mathrm{SIA}_{\mathrm{AMSR-E}} - \mathrm{SIA}_{\mathrm{SSMIS}}} \quad (2)$$

are shown. Determination coefficients, R^2, for three ROIs are greater than 0.99, as expected.

In Table 1, the three slope values, being close to unity, suggest that the use of the above adjustment procedure was not critical; on the contrary, the application of a linear regression for the transition period from AMSR-E to AMSR-2 is needed, as the simple insertion of SSMIS data would produce a SIA underestimation. A new linear regression, using common data for both SSMIS and AMSR-2, was applied:

$$\mathrm{SIA}_{\mathrm{AMSR}} = c_0 + c_1 \mathrm{SIA}_{\mathrm{SSMIS}} \quad (3)$$

Results, analogous to those of Table 1, are shown in Table 2; determination coefficients, R^2, are still larger than 0.99.

Results

Maximum and minimum annual values

The SIA monthly time series, together with the regression lines for maximum and minimum values, are shown in Figure 4 for the three ROIs.

The slope values $\beta_{\mathrm{max,ROI}}$ and $\beta_{\mathrm{min,ROI}}$ (ROI $= 1, \ldots, 3$) with their standard errors, $\mathrm{se}_{\mathrm{max/min,ROI}}$, are reported in Table 3. The two-sided null hypothesis $H_0 : \beta_{\mathrm{max/min,ROI}} = 0$ was tested with the t-statistic, $t = (\beta_{\mathrm{max/min,ROI}}/\mathrm{se}_{\mathrm{max/min,ROI}})$. The null hypothesis should be rejected if the corresponding p-value is smaller than a selected significance level.

Observation of Table 3 leads to the following considerations:

- All maximum and minimum values, except Greenland Sea minimums, show a statistically significant trend at significance level $\alpha = 0.05$.
- The variability of maximum annual values for ROI2 is greater than for ROI1 and ROI3, particularly before 2003 as can be seen in Figure 4.
- For all ROIs, minimum values are always observed in August or September; most of them, for ROI1 and ROI3, occur in September while those for ROI2 mainly occur in August (Table 4). Note that for ROI3, the

Table 1. Regression coefficients, mean area difference and standard deviation for the overlap period between AMSR-E and SSM/I products for each ROI.

	c_0 (10^3 km^2)	c_1	md (10^3 km^2)	sd (10^3 km^2)
ROI1	− 209.55	1.02	9.69	231.77
ROI2	− 37.15	1.07	− 12.04	19.92
ROI3	− 18.89	1.04	40.95	29.19

Table 2. Regression coefficients, mean area difference and standard deviation for the overlap period between AMSR-2 and SSMIS products for each ROI.

	c_0 (10^3 km^2)	c_1	md (10^3 km^2)	sd (10^3 km^2)
ROI1	− 439.96	1.22	1.20×10^3	0.66×10^3
ROI2	22.19	1.19	75.72	27.98
ROI3	− 17.84	1.05	37.74	28.71

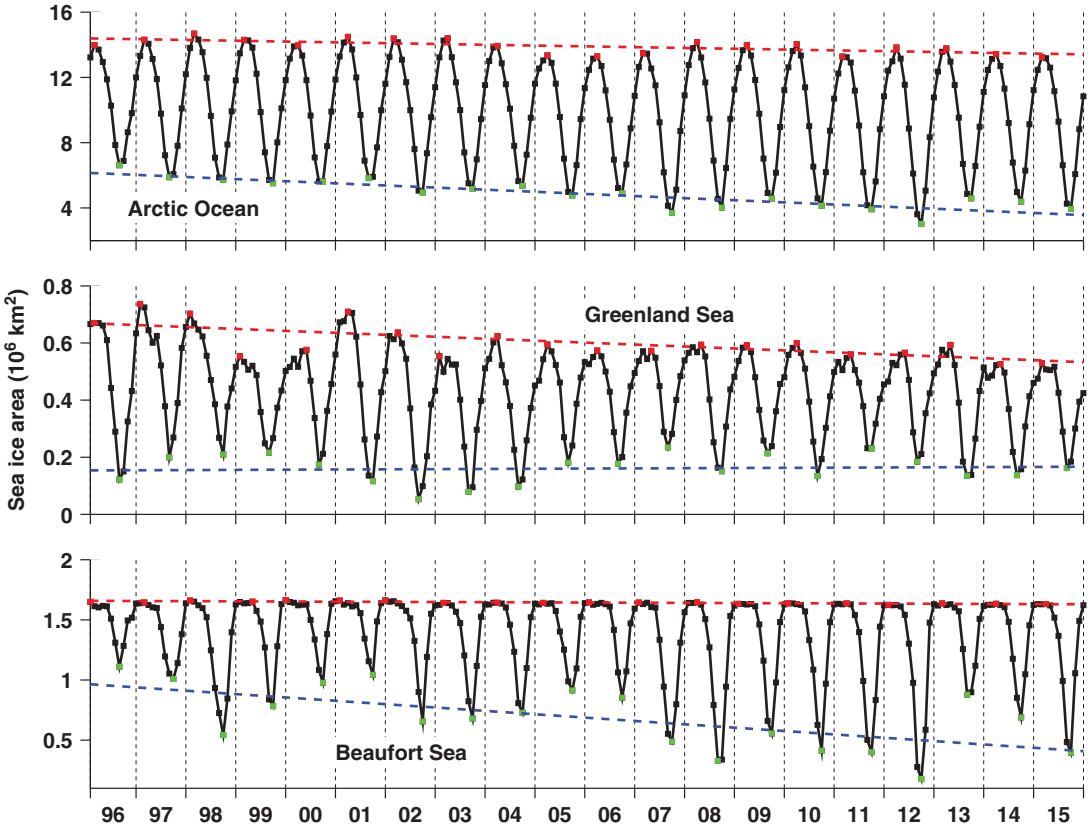

Figure 4. Monthly SIA with maximum and minimum annual trends. Top: whole.

trend of minimum values seems to follow a periodic cycle of some 4–5 years; although less evident, the periodic cycle for ROI2 is about 6 years.

- Maximum values were always observed in February and March for ROI1, between January and May for ROI2, and between January and March for ROI3, except in 2000 and 2002 (December) and 1999 (April). After 1999, maximum values for ROI2 tend to occur later than for ROI3 (see Table 4).
- In 2000 and in 2012, i.e. in correspondence with SIA minimum, maximum values in the Greenland Sea were observed in May.

Table 3. SIA linear trends (10^3 km^2 year^{-1}) and standard errors of annual maximums, annual minimums and monthly anomalies, for Arctic Ocean, Greenland Sea and Beaufort Sea (1996–2015).

	ROI1	ROI2	ROI3
Ann. max.	-49.1 ± 13.4	-6.8 ± 1.7	-1.4 ± 0.3
Ann. min.	-129.7 ± 18.2	0.7 ± 2.0	-27.9 ± 8.2
Monthly anom.	-72.4 ± 4.4	-3.9 ± 0.6	-8.4 ± 1.5

Data in boldface are statistically significant at $a = 0.05$.

Table 4. Months, for each year, in which maximum and minimum SIA was observed.

	ROI1		ROI2		ROI3	
Year	MAX	MIN	MAX	MIN	MAX	MIN
1996	FEB	AUG	FEB	AUG	JAN	AUG
1997	FEB	AUG	JAN	AUG	FEB	SEP
1998	FEB	SEP	JAN	SEP	JAN	SEP
1999	FEB	SEP	JAN	AUG	APR	SEP
2000	MAR	SEP	MAY	AUG	DEC	SEP
2001	MAR	AUG	MAR	SEP	JAN	SEP
2002	FEB	SEP	MAR	AUG	DEC	SEP
2003	MAR	SEP	JAN	AUG	FEB	SEP
2004	MAR	SEP	MAR	AUG	MAR	SEP
2005	MAR	SEP	MAR	AUG	FEB	SEP
2006	MAR	SEP	MAR	AUG	JAN	SEP
2007	FEB	SEP	APR	AUG	JAN	SEP
2008	MAR	SEP	APR	SEP	MAR	AUG
2009	MAR	SEP	MAR	AUG	JAN	SEP
2010	MAR	SEP	MAR	AUG	JAN	SEP
2011	FEB	SEP	APR	SEP	MAR	SEP
2012	MAR	SEP	MAY	AUG	JAN	SEP
2013	MAR	SEP	APR	AUG	FEB	AUG
2014	MAR	SEP	APR	AUG	MAR	SEP
2015	FEB	SEP	FEB	AUG	MAR	SEP

Monthly SIA anomalies

In order to minimize the intra-annual seasonal variations, the monthly anomaly trends, obtained by subtracting the monthly climatological averages from each monthly average (Comiso & Nishio, 2008), were computed and are shown in Figure 5, with Table 3 reporting their slope values.

With regard to Figure 5 and Table 3, and comparing the results to those of other authors, it is possible to say:

- Negative trends of monthly anomalies are all statistically significant at virtually any statistical significant level α.
- The two main negative anomalies of the entire Arctic Ocean (ROI1) occurred in 2007 and in 2012, while in the Beaufort Sea, they occurred in 2008 and 2012. The need to speculate about

different physical processes for the 2007 and 2012 events is clear: in 2012, the cause may have been the arrival of a strong storm over the central Arctic, which produced the separation and the melting of a large expanse of ice (Parkinson & Comiso, 2013); for the 2007 decline, instead, the contributions of cloud and radiation anomalies were decisive (Kay, L'Ecuyer, Gettelman, Stephens, & O'Dell, 2008).

- For each investigated region, monthly SIA anomalies were compared to the monthly surface air temperature anomalies. The comparison for the three ROIs is shown in Figure 5 where, to improve clarity, a moving average smoothing was applied and the linear trend was removed. Surface air temperature data were retrieved from the NCEP-NCAR R1 archive (Kalnay et al., 1996). Large temperature anomalies are observed in correspondence of the large negative SIA anomalies, as for the Beaufort Sea region (Figure 5) in 1998, 2007 and 2012. Besides, it is interesting to note the strong anticorrelation for ROI2, not so apparent for ROI3, due to the low anomaly values during the 2002–2005 period; ROI2, in the same period, shows a high annual relative range (Figure 5). Correlation coefficients between SIA and temperature anomalies for each regions are -0.40, -0.29 and -0.31, respectively, and are all statistically significant at significance level $\alpha = 0.05$.
- Despite the different analysed periods, a comparison of SIA value trends obtained by other authors is shown in Table 5, where column 5 reports the SIA trend values for 1979–2010 and 1979–1996, derived from 32 years of SSM/I-SSMIS observations by Cavalieri and Parkinson (2012); a rough estimation of the trends for the period 1996–2010 gives for ROI1, $-70.7\,\mathrm{km^2\,year^{-1}}$, for ROI2, $-5.4^3\,\mathrm{km^2\,year^{-1}}$, values very close to the one reported in this paper. In Comiso et al. (2008), the

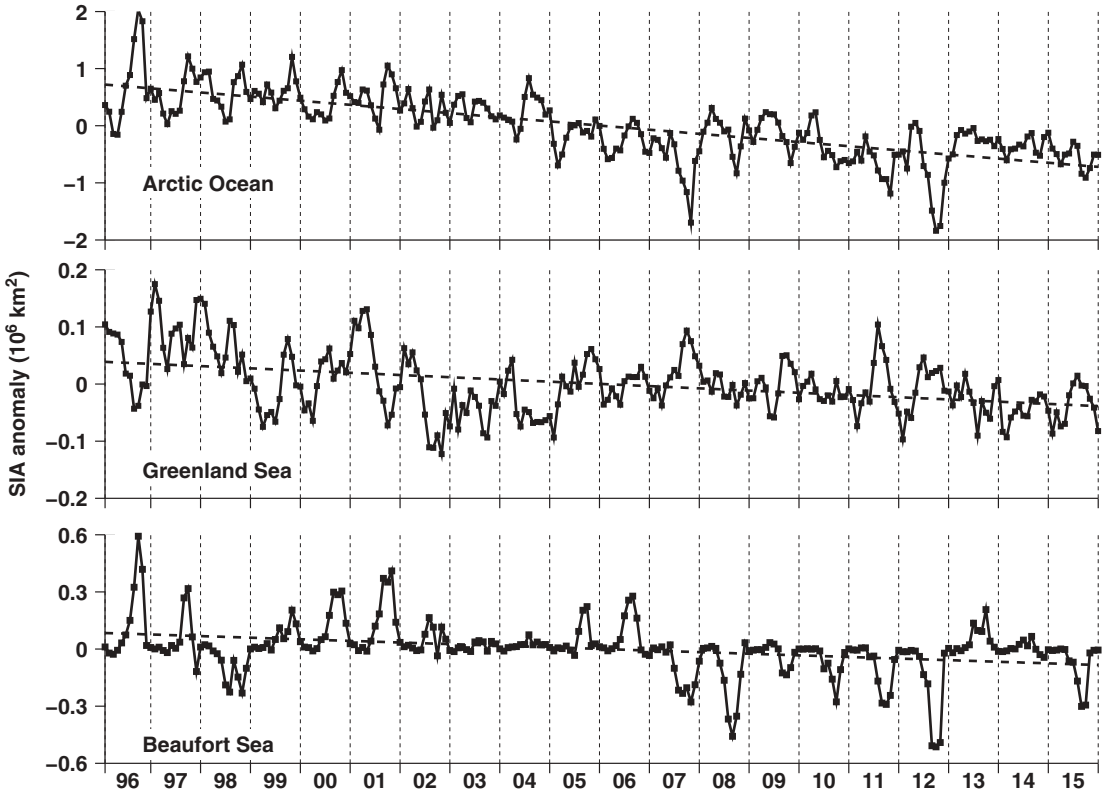

Figure 5. Monthly SIA anomaly trends. Top: whole Arctic Ocean; middle: Greenland Sea; bottom: Beaufort Sea.

Table 5. SIA monthly anomaly trend ($10^3\,\mathrm{km^2\,year^{-1}}$) with the standard error comparison.

	ROI1	ROI2
This work	(1996–2015) -72.4 ± 4.4	(1996–2013) -3.9 ± 0.6
Comiso and Nishio (2008)	(1978–2007) -42.8 ± 2.0	
Comiso et al. (2008)	(1978–1996) -33.0 ± 4.1	
	(1996–2007) -110.1 ± 8.0	
	(1978–2007) -46.8 ± 2.1	
Cavalieri and Parkinson (2012)	(1979–2010) -49.6 ± 4.0	(1979–2010) -3.7 ± 0.9
	(1979–1996) -29.3 ± 8.3	(1979–1996) -2.1 ± 2.3
Parkinson and Cavalieri (2008)	(1979–2006) -41.0 ± 4.3	(1979–2006) -4.2 ± 1.1

In brackets, the corresponding analysed period.

trend for ROI1 in the period 1996–2007 appears higher than the one reported by Parkinson and Cavalieri (2008) for the period 1979–2006.
- Correlations between monthly SIA anomalies and monthly Southern Oscillation Index (SOI) for the three regions are -0.14, -0.08 and -0.14, respectively; p-values suggest a significant statistical correlation between SIA and SOI for ROI1 and ROI3.

Discussion and conclusions

Some conclusions based on the results of the previous section are

- Trend comparison (Table 5) confirms a considerable compatibility between SIA computation using NSIDC and IUP data sets, although obtained from independent observations; the time series of the other authors in Table 5 are based on the Bootstrap (Comiso, 2012) and NASA Team (Cavalieri & Parkinson, 2012) algorithms, respectively, which both use the 19 and 37-GHz channels, whereas, as already stated, the ASI algorithm used here uses the 89-GHz brightness temperatures.
- All trends, except for minimum values in the Greenland Sea ($0.7 \pm 2.010^3\,km^2\,year^{-1}$), are negative: with the null hypothesis of trend's absence, all p-values are much lower than the significance level $\alpha = 0.05$. The apparent slightly increasing SIA in the Greenland Sea is most likely due to the continuous oceanic outflow through the Fram Strait.
- For ROI2, summer minimum values are occurring about one month earlier (August) than ROI1 and ROI3 (September).
- In ROI3, the maximum values are often persistent for 6–7 months.

The relevant result of this study is provided by Figure 4 which shows, for the 20 years under analysis, an increase of SIA in the Greenland Sea, in contrast to what has occurred in the Arctic Ocean as a whole and, to a greater extent, in the Beaufort Sea. Studies on the ice loss in the Beaufort Sea (Hutchings & Rigor, 2012; Kwok & Cunningham, 2010; Steele, Dickinson, Zhang, & Lindsay, 2015) have shown how extreme cyclonic circulations of the recent years have produced a decrease of the ice age and how this resulted in ice within the central Beaufort Gyre being less than 5 years old and hence more easily subject to melting. For the Greenland Sea, it has been demonstrated that the large flux of ice from the Arctic Basin through the Fram Strait, with its injection of freshwater to the North Atlantic (De Steur et al., 2009; Kwok, Cunningham, & Pang, 2004), leads to an increased SIA and to a rapid decline in the ice area of the Arctic. Even if formulated for the Antarctic Ocean, the hypothesis of King (2014) may apply to Arctic regions of different morphology. For the reasons explained, the Beaufort Sea, a closed sea, has seen a marked decline of ice in the recent years while in the Greenland Sea, an open sea, the SIA tends to grow.

Acknowledgements

We acknowledge the support of the European Union ICE-ARC project (Ice, Climate and Economics – Arctic Research on Change), contract 603887. We are also grateful to

- the Inst. of Environmental Physics of the University of Bremen for providing the ARCTIC SIC data set through its website (http://www.iup.uni-bremen.de:8084/amsr2/);
- the NCEP for the Reanalysis Data provided by the NOAA/OAR/ESRL PSD, Boulder, Colorado, USA, through its website (http://www.esrl.noaa.gov/psd/).

Disclosure statement

No potential conflict of interest was reported by the authors.

Funding

This work was supported by the Seventh Framework Programme [ICE-ARC project 603887].

References

Cavalieri, D.J., & Parkinson, C.L. (2012). Arctic sea ice variability and trends, 1979–2010. *The Cryosphere*, *6*, 881–889. doi:10.5194/tc-6-881-2012

Comiso, J.C. (2012). Large decadal decline of the Arctic multiyear ice cover. *Journal of Climate*, *25*, 1176–1193. doi:10.1175/JCLI-D-11-00113.1

Comiso, J.C., & Hall, D.K. (2014). Climate trends in the Arctic as observed from space. *Wires Climate Change*, *5*, 389–409. doi:10.1002/wcc.277

Comiso, J.C., & Nishio, F. (2008). Trends in the sea ice cover using enhanced and compatible AMSR-E, SSM/I and SMMR data. *Journal of Geophysical Research*, *113*, C02S07. doi:10.1029/2007JC004257

Comiso, J.C., Parkinson, C.L., Gersten, R., & Stock, L. (2008). Accelerated decline in the Arctic sea ice cover. *Geophysical Research Letters*, *35*, L01703. doi:10.1029/2007GL031972

De Steur, L., Hansen, E., Gerdes, R., Karcher, M., Fahrbach, E., & Holfort, J. (2009). Freshwater fluxes in the east Greenland current: A decade of observations. *Geophysical Research Letters*, *36*, L23611. doi:10.1029/2009GL041278

Hutchings, J.K., & Rigor, I.G. (2012). Role of ice dynamics in anomalous ice conditions in the Beaufort Sea during

2006 and 2007. *Journal of Geophysical Research*, *117*, C00E04. doi:10.1029/2011JC007182

Kaleschke, L., Lüpkes, C., Vihma, T., Haarpaintner, J., Bochert, A., Hartmann, J., & Heygster, G. (2001). SSM/I sea ice remote sensing for mesoscale ocean-atmosphere interaction analysis. *Canadian Journal of Remote Sensing*, *27*, 526–537. doi:10.1080/07038992.2001.10854892

Kalnay, E., Kanamitsu, M., Kirtler, R., Collins, W., Deaven, D., Gandin, L., … Joseph, D. (1996). The NCEP/NCAR 40-year reanalysis project. *Bulletin of the American Meteorological Society*, *77*, 437–471. doi:10.1175/1520-0477(1996)077<0437:TNYRP>2.0.CO;2

Kay, J.E., L'Ecuyer, T., Gettelman, A., Stephens, G., & O'Dell, C. (2008). The contribution of cloud and radiation anomalies to the 2007 Arctic sea ice extent minimum. *Geophysical Research Letters*, *35*, L08503. doi:10.1029/2008GL033451

King, J. (2014). Climate science: A resolution of the Antarctic paradox. *Nature*, *505*, 491–492. doi:10.1038/505491a

Kwok, R., & Cunningham, G.F. (2010). Contribution of melt in the Beaufort Sea to the decline in Arctic multi-year sea ice coverage: 1993–2009. *Geophysical Research Letters*, *37*, L20501. doi:10.1029/2010GL044678

Kwok, R., Cunningham, G.F., & Pang, S.S. (2004). Fram Strait sea ice outflow. *Journal of Geophysical Research*, *109*, C01009. doi:10.1029/2003JC001785

Liu, Y., Key, J.R., & Wang, X. (2009). Influence of changes in sea ice concentration and cloud cover on recent Arctic surface temperature trends. *Geophysical Research Letters*, *36*, L20710. doi:10.1029/2009GL040708

Meier, W.N., Stroeve, J., & Fetterer, F. (2007). Whither Arctic sea ice? A clear signal of decline regionally, seasonally and extending beyond the satellite record. *Annals of Glaciology*, *46*, 428–434. doi:10.3189/172756407782871170

Parkinson, C.L., & Cavalieri, D.J. (2008). Arctic sea ice variability and trends, 1979-2006. *Journal of Geophysical Research*, *113*, C07003. doi:10.1029/2007JC004558

Parkinson, C.L., Cavalieri, D.J., Gloersen, P., Zwally, H.J., & Comiso, J.C. (1999). Arctic sea ice extents, areas, and trends, 1978-1996. *Journal of Geophysical Research*, *104* (C9), 20837–20856. doi:10.1029/1999JC900082

Parkinson, C.L., & Comiso, J.C. (2013). On the 2012 record low Arctic sea ice cover: Combined impact of preconditioning and an August storm. *Geophysical Research Letters*, *40*, 1356–1361. doi:10.1002/grl.50349

Serreze, M.C., & Barry, R.G. (2014). *The Arctic climate system* (2nd ed.). New York: Cambridge Univ. Press.

Spreen, G., Kaleschke, L., & Heygster, G. (2008). Sea ice remote sensing using AMSR-E 89-GHz channels. *Journal of Geophysical Research*, *113*, C02S03. doi:10.1029/2005JC003384

Steele, M., Dickinson, S., Zhang, J., & Lindsay, R.W. (2015). Seasonal ice loss in the Beaufort Sea: Toward synchrony and prediction. Journal of Geophysical Research Oceans, *120*, 1118–1132. doi:10.1002/2014JC010247

Stroeve, J.C., Serreze, M.C., Holland, M.M., Kay, J.E., Malanik, J., & Barrett, A.P. (2012). The Arctic's rapidly shrinking sea ice cover: A research synthesis. *Climatic Change*, *110*, 1005–1027. doi:10.1007/s10584-011-0101-1

Toudal, L. (1999). Ice extent in the Greenland Sea 1978-1995. *Deep-Sea Research II*, *46*, 1237–1254. doi:10.1016/S0967-0645(99)00021-1

Vinnikov, K.Y., Cavalieri, D.J., & Parkinson, C.L. (2006). A model assessment of satellite observed trends in polar sea ice extents. *Geophysical Research Letters*, *33*, L05704. doi:10.1029/2005GL025282

Vinnikov, K.Y., Robock, A., Stouffer, R.J., Walsh, J.E., Parkinson, C.L., Cavalieri, D.J., … Zakharov, V.F. (1999). Global warming and northern hemisphere sea ice extent. *Science*, *286*, 1934–1937. doi:10.1126/science.286.5446.1934

Wang, X., Key, J., Liu, Y., Fowler, C., Maslanik, J., & Tschudi, M. (2012). Arctic climate variability and trends from satellite observations. *Advances in Meteorology*, *2012*, 1–22. doi:10.1155/2012/505613

Zwally, H.J., Comiso, J.C., Parkinson, C.L., Campbell, F.D., Carsey, F.D., & Gloersen, P. (1983). *Antarctic sea ice 1973-1976 from satellite passive microwave observations*. Spec. Publ., 459. Washington, DC: NASA.